

Article

Testing and Analysis on the Spatial and Temporal Distribution of Light Intensity and CO₂ Concentration in Solar Greenhouse

Chunhui Zhang ^{1,†}, Haiyang Liu ^{1,†}, Chunguang Wang ¹, Zheyong Zong ^{1,2,*}, Haichao Wang ³, Xiaodong Zhao ⁴, Shuai Wang ¹ and Yanan Li ¹

¹ College of Mechanical and Electrical Engineering, Inner Mongolia Agricultural University, Hohhot 010018, China

² Key Laboratory of Biopesticide Creation and Resource Utilization of Universities, Hohhot 010018, China

³ College of Energy and Transportation Engineering, Inner Mongolia Agricultural University, Hohhot 010018, China

⁴ Xilingol Power Supply Company, Xilinhot 026000, China

* Correspondence: zongzheyong@imau.edu.cn

† These authors contributed equally to this work.

Abstract: Greenhouses, as important parts of facility agriculture, can reduce the restrictions on agricultural production imposed by the natural environment and make rational and efficient use of production resources. We conducted long-term, continuous testing of temperature, humidity, light intensity, and CO₂ concentration parameters in a heliostat greenhouse in the central and western parts of the Inner Mongolia Autonomous Region, a cold and arid region of northern China. A large amount of data was processed by statistical observation, simulation analysis, and 3D reconstruction to obtain the overall distribution, variation pattern, and mathematical model of the regional greenhouse environment in time and space. The results show that the temperature, humidity, light intensity, and CO₂ concentration in the greenhouse have significant daily variation patterns, that there are strong coupling relationships between light intensity–CO₂ concentration–time and indoor temperature–light intensity–CO₂ concentration, that the coefficients of determination (R^2) of the mathematical models are 0.88 and 0.89, and that the standard errors (RMSE) are 49.67 ppm and 45.30 ppm, respectively. The environmental parameters were fitted with high accuracy in order to provide scientific data for the cultivation of heliostats in the region.

Keywords: solar greenhouse; environmental parameters; spatial and temporal distribution; modeling



Citation: Zhang, C.; Liu, H.; Wang, C.; Zong, Z.; Wang, H.; Zhao, X.; Wang, S.; Li, Y. Testing and Analysis on the Spatial and Temporal Distribution of Light Intensity and CO₂ Concentration in Solar Greenhouse. *Sustainability* **2023**, *15*, 7001. <https://doi.org/10.3390/su15087001>

Academic Editors: Hassan Abdalla and Arya Assadi Langroudi

Received: 20 February 2023

Revised: 13 April 2023

Accepted: 20 April 2023

Published: 21 April 2023



Copyright: © 2023 by the authors. Licensee MDPI, Basel, Switzerland. This article is an open access article distributed under the terms and conditions of the Creative Commons Attribution (CC BY) license (<https://creativecommons.org/licenses/by/4.0/>).

1. Introduction

As major vehicles for modern agriculture in China, solar greenhouses can provide an annual supply of agricultural products and are an important part of agricultural production in cold and arid regions of northern China [1,2]. Among various factors, the microclimate environment inside solar greenhouses is the most direct factor affecting crop growth and development [3]. This environmental parameter is characterized by strong time variability, poor linearity, and strong coupling, and is susceptible to the influence of uncertainties such as external environmental changes and greenhouse building structures. Planting and management without knowledge of the spatial and temporal distribution of temperature inside the greenhouse is highly susceptible to low crop yield, disease, and even death [4,5]. Therefore, exploring and mastering the differences in spatial and temporal distributions of small environmental parameters inside greenhouses is the first task to improve crop yields, rationalize crop planting structures, and improve environmental control strategies, which is of great significance for the precise development of modern agriculture.

At this stage, foreign researchers and scholars have studied the temperature, light intensity, and CO₂ concentration in greenhouses. Existing studies have found that greenhouse indoor temperature is related to outdoor temperature, ventilation rate, solar radiation,

greenhouse structure, and indoor relative humidity [6–8]. In terms of greenhouse indoor temperature, Hamad et al. [9] developed a model of greenhouse interior temperature for Tunisian greenhouses which better described the evolution of greenhouse interior temperature. Cayli [10] conducted a study on the mulching structure of Turkish greenhouses and showed that the thermal uniformity of double-layer polyethylene (PE) mulched greenhouses was better than that of single-layer PE mulched ones. He et al. [11], based on the study of Yang from Shenyang Agricultural University [12], collected and analyzed different horizontal and vertical temperatures and ground temperatures inside greenhouses for northern greenhouses and summarized the internal temperature variation patterns. Le et al. [13] investigated the temperature variation patterns of greenhouses for strawberry production in Langfang City. Meanwhile, domestic and foreign researchers have analyzed the light intensity inside greenhouses. Zhang et al. [14] established a light environment model of a heliostat greenhouse in the west corridor of China. Mobtaker et al. [15] compared the absorption effect of solar radiation by various greenhouse forms, and the study showed that solar radiation directly influenced greenhouse temperature while the building structure of the greenhouse affected the absorption of solar radiation by the greenhouse. Lv et al. [16] explored the trends of light intensity and indoor temperature in greenhouses. Gao et al. [17] studied the characteristics of sunlight and its changing pattern in a Henan Xinxiang City greenhouse, giving the relationship between indoor and outdoor light intensity and transmittance in different months. Tong et al. [18] tested the light intensity in the middle of the inside of a liao-shen type I sunlight greenhouse, giving only the light intensity and transmittance at noon on different days. In a study of greenhouse CO₂ concentration, Zhang et al. [19] analyzed the distribution of temperature for U.S. greenhouses and monitored CO₂ concentration accordingly. The results of Yang et al.'s [20] analysis of CO₂ concentration in greenhouses showed that there were differences in CO₂ concentration at different heights and locations without ventilation. At this stage, bionomics and nature-inspired design are receiving attention from a wide range of scholars [21], and designing engineered systems that are symbiotic with nature (i.e., light patterns here, evaporated CO₂) and engineered systems (shape of the roof/exterior walls) is viewed as beneficial for solving the bottleneck of greenhouse structural design.

Although a large number of scholars at home and abroad have acquired and analyzed the spatial heterogeneity of greenhouse environmental parameters to provide a basis for the spatial management of agro-meteorological parameters, they have mainly focused on spatial and temporal analysis and the modeling of single environmental factors, and the influence of meteorological conditions in the area where the greenhouse is located on the distribution of environmental parameters inside the greenhouse is often ignored. The indoor and outdoor environments of greenhouses vary greatly among different greenhouse structures and regions. In particular, greenhouse environmental research on the climatic characteristics of northern China's cold and arid regions is relatively weak, and there is a lack of basic data on the spatial and temporal distribution of greenhouse environments in this region, especially regarding analysis and research on the coupled distribution of multiple environmental factors in a typical heliostat in northern China.

Therefore, in this paper, a typical heliostat in the central and western regions of the Inner Mongolia Autonomous Region was selected as the experimental object to monitor the internal temperature, humidity, light intensity, and CO₂ concentration in the heliostat during the winter alpine period, with the aim of drawing the overall change curve and determining the daily change pattern. The spatial and temporal distributions of light intensity and CO₂ concentration in different height planes and typical longitudinal profiles were analyzed, the three-dimensional distributions of light intensity and CO₂ concentration were reconstructed, and a three-dimensional mathematical model was established. Finally, the coupling relationship between the parameters and the main factors affecting the changes of indoor environmental parameters were obtained. This can provide a theoretical basis for optimizing greenhouse structures and proposing reasonable greenhouse crop planting layouts and greenhouse environmental control strategies.

2. Materials and Methods

2.1. Test Site

Solar greenhouses are mainly used in winter, spring, and autumn, so our experiments were conducted in winter from December to February. The test greenhouse was selected from the No. 4 greenhouse of Hailiutu Science and Technology Park of Inner Mongolia Agricultural University, located in the territory of Hailiutu Village, Beish Axis Township, Tuzuo Banner, Hohhot City, with the geographical coordinates of $111^{\circ}22'30''$ E, $40^{\circ}41'30''$ N and an altitude of 905 m. The solar greenhouse is oriented east–west, 70 m long, and 5° south by west. The ridge height is 4 m, the span is 8 m, and the lighting angle is $20^{\circ}17'$; the wall is made of brick sandwiched between earth, the rear insulation wall is 2.7 m high and 1.4 m thick, and the east–west hill wall is a brick wall that is 0.5 m thick. The light-transmitting covering material is PVC film. The PVC thickness is 0.06–0.12 mm, while the transmittance of new mold light is about 80%, ultraviolet 20%, visible 86–88%, and near infrared 93–94%. The mid-infrared is 72 and the far-infrared is 40. The greenhouse has better insulation, is 90% dustproof when new and 50% dustproof after 1 year, has a tensile strength of 19–23 Mpa, has an elongation of 250–290%, and has a right angle tear of 810–877 N/cm. Its impact strength is $14.5/\text{cm}^2$ and the specific gravity $1.03 \text{ g}/\text{cm}^2$. The insulation cover material for the outer skin is made of a rainproof silk inner core fiber and a cotton curtain; the cotton curtain thickness is 2–3 cm, the density is between $200 \text{ g}/\text{m}^2$ – $300 \text{ g}/\text{m}^2$, with good thermal insulation performance, and the light transmission rate is between 30–40%. The load-bearing structure is a double skeleton diagonally drawn steel skeleton; the interior has a 0.6 m wide concrete aisle near the back wall side. It is shown in Figure 1.



Figure 1. Experimental solar greenhouse: (a) Appearance; (b) Inside.

2.2. Data Acquisition

2.2.1. Environmental Monitoring Systems in Greenhouses

The environmental detection sensors inside the greenhouse mainly include environmental temperature and humidity sensors (SHT31, Sensirion, Stfa, Switzerland), soil temperature and humidity sensors (HSTL-10STR, Huakong, Beijing, China), light sensors (RS-GZ-NO1-2, JD Renke, Shandong, China), and carbon dioxide concentration sensors (RS-CO₂-NO1-2, JD Renke, Shandong, China) to realize the collection of temperature, humidity, light intensity, carbon dioxide concentration, and soil temperature and humidity inside the greenhouse. Each sensor is connected to the greenhouse environmental acquisition node using an RS458 communication interface and Mdobus protocol. The greenhouse environmental acquisition node is mainly composed of a dual serial microcontroller (STC12C5A60S2), a wireless data transmission module, and an RS485 serial communication circuit, which is responsible for the establishment of wireless communication and control of the sensor groups, as well as the acquisition, processing, and packaging of environmental parameters and wireless transmission tasks. Each greenhouse environmental collection

node adopts a star-type wireless self-organizing data transmission network to realize data interaction with the greenhouse environmental parameters autonomous measurement and control system. The greenhouse environmental parameters independent measurement and control system is mainly composed of a Mitsubishi PLC (FX-2N series) and MCGS configuration touch screen, which realizes the functions of real-time aggregation and centralized display of data, independent processing, and regulation of environmental parameters; reception of remote control instructions, centralized displays, and classification and storage of parameters; and real-time change curve drawing and reorganization and forwarding of data packets. The environmental data inside the greenhouse are summarized and packaged by the greenhouse environmental parameters' independent measurement and control system, and the data are uploaded to the server in real time by using GPRS data transmission equipment to build a long-distance wireless communication network. The final data are collected and processed by LabVIEW client data processing software, which communicates with the remote server through TCP protocol, realizing the functions of real-time collection and processing, remote data transmission, and aggregate analysis of environmental parameters inside the greenhouse group, etc. The greenhouse environmental parameters collection system is shown in Figure 2. The greenhouse environmental monitoring system records data once every 1 min.

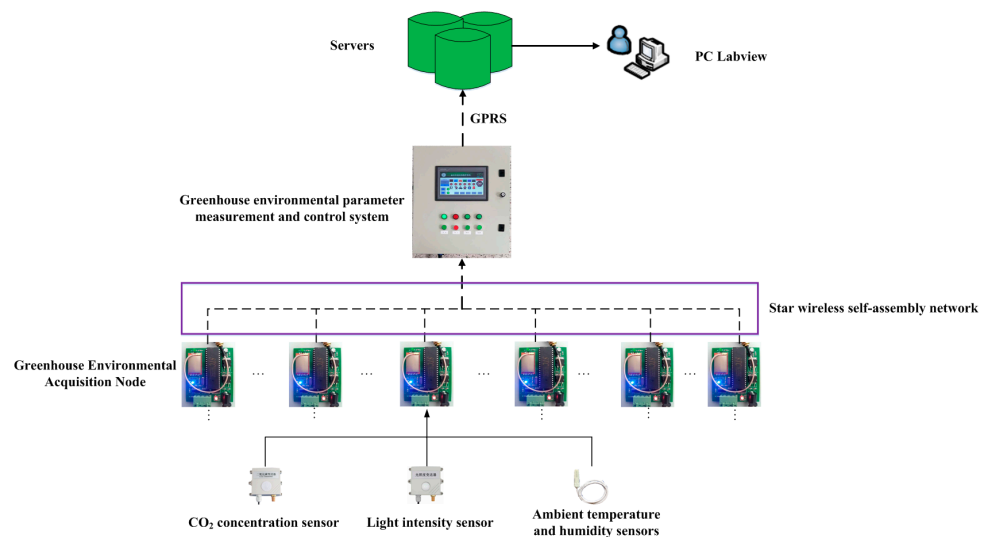


Figure 2. Greenhouse environmental parameter acquisition system.

2.2.2. Greenhouse External Environment Monitoring Device

We installed a set of JZH-1 outdoor environment monitoring weather stations from Jinzhou Sunshine Weather Co., Ltd. (Jinzhou, China) outside the greenhouse, which can collect real-time weather data such as outdoor ambient temperature, ambient humidity, dew point, air pressure, wind speed, wind direction, and radiation value, as shown in Figure 3. The air temperature and humidity sensors are horizontally installed at 1.5 m on vertical ground. The range of the air humidity sensor is 0~100%, its accuracy is $\pm 2\%$, and its resolution is 0.1% the range of the air temperature sensor is $-40\sim 80\text{ }^{\circ}\text{C}$, its accuracy is $\pm 0.2\text{ }^{\circ}\text{C}$, and its resolution is $0.1\text{ }^{\circ}\text{C}$. The illuminance sensor range is 0~200,000 Lux, its accuracy is $\pm 2\%$, and its resolution is 1 Lux; it is installed horizontally at 1.5 m on vertical ground. The wind speed sensor range is 0~45 m/s, its accuracy is $\pm 0.2\text{ m/s}$, and its resolution is 0.1 m/s ; it is installed horizontally at 3 m on vertical ground. The wind direction sensor range is $0\sim 360^{\circ}$, its accuracy is $\pm 0.1^{\circ}$, and its resolution is 0.1° ; it is installed horizontally at 3 m on vertical ground.

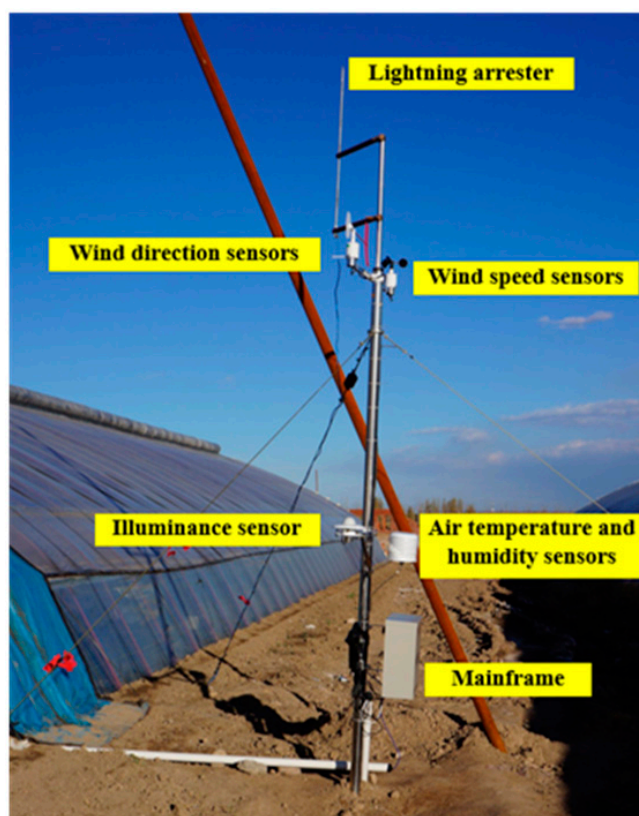


Figure 3. Outdoor environmental monitoring weather station.

2.3. Test Program

2.3.1. Horizontal Layout Plan

In order to study the overall distribution and mutual effects of temperature, humidity, light intensity, and CO₂ concentration in a solar greenhouse at the same horizontal height, we selected a typical horizontal height plane of 0.5 m from the ground surface as a reference basis for the overall test and analysis of temperature, humidity, light intensity, and CO₂ concentration inside the greenhouse.

During the test, the interior area of the greenhouse was divided into 20 equal rectangular test areas (length \times width: 7 m \times 4 m). A test point was set at the geometric center of each area, and one light intensity sensor, one CO₂ concentration sensor, one temperature and humidity sensor, and one wireless data collector were placed at each test point. A total of 20 ambient temperature and humidity sensors, 8 light intensity sensors, and 8 CO₂ concentration sensors were arranged on the test plane, making a total of 36 sensors. To improve the reliability of the test data, only ambient temperature and humidity sensors were arranged in areas 1 and 10; only ambient temperature and humidity sensors, light intensity sensors, and CO₂ concentration sensors were arranged in areas 2 to 9; and only ambient temperature and humidity sensors were arranged in areas 11 to 20. During the test, the light intensity sensor was kept horizontal. Outdoor environmental monitoring weather stations were arranged 1.5 m southward from the center point of the front roof of the greenhouse to collect outdoor temperature, humidity, light intensity, wind speed, and other environmental parameters. The measurement point layout schematic is shown in Figure 4a, and the sensor arrangement is shown in Figure 4b.

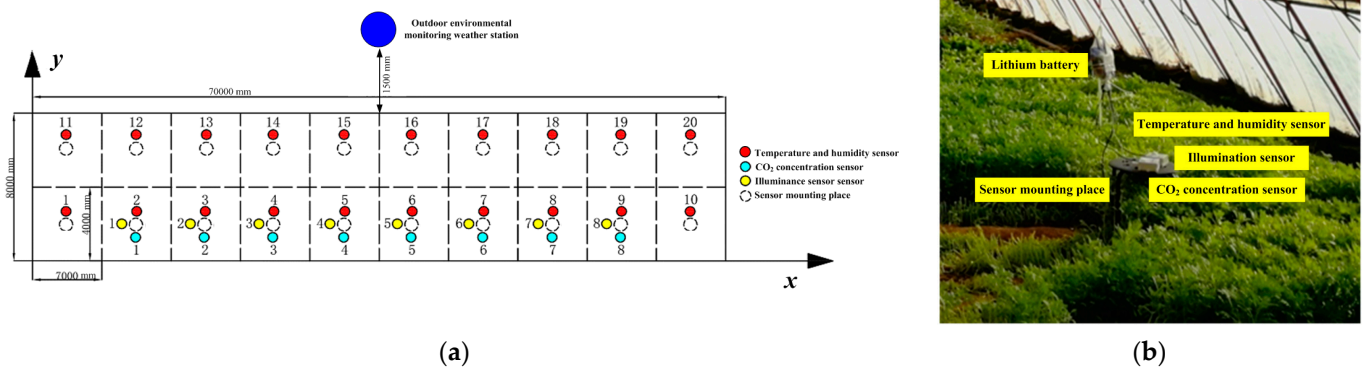


Figure 4. Division of the internal area of the solar greenhouse and layout of the sensors in the horizontal direction: (a) Schematic diagram; (b) Physical image.

2.3.2. Vertical Layout Plan

To study the distribution patterns of temperature, humidity, light intensity, and CO₂ concentration in the heliostat at different heights, and to reduce the measurement errors caused by the greenhouse structure and external insulation equipment, we arranged the sensors in a vertical direction 5 m west of the center of the greenhouse interior. As the lowest point of the front roof, the ridge height position and the back wall of the greenhouse have an important influence on the distribution of environmental parameters inside the greenhouse. According to the degree of significant changes in the distribution of environmental parameters, we took the location of the No. 1 environmental temperature and humidity measurement point as the reference point, and we selected distances from the reference point of 0 m, 1.75 m, 3.5 m, 5.25 m, 7 m, and 8 m along the horizontal direction, respectively. We laid the measurement points upward along the vertical direction. The sensors were spaced at 0.9 m per layer, and a total of 4 layers were used to measure temperature, humidity, light intensity, and CO₂ concentration at different heights inside the greenhouse. The sensor layout is shown in Figure 5.

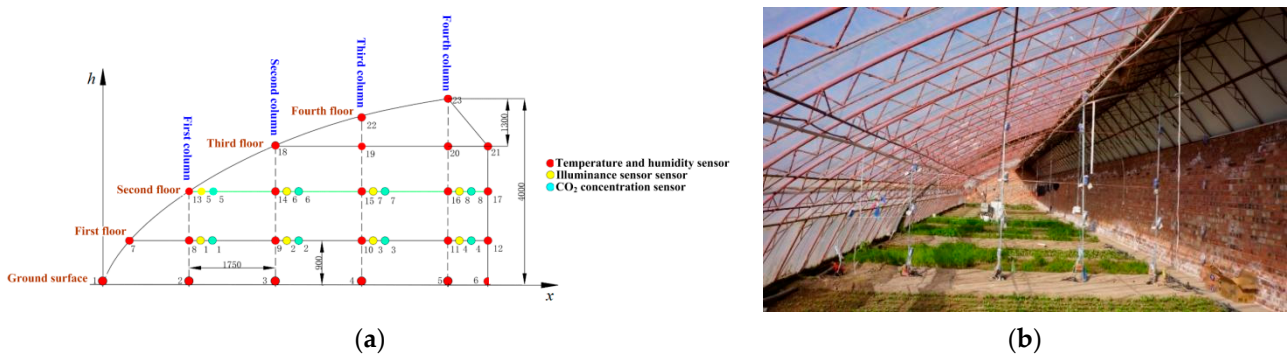


Figure 5. Sensor longitudinal layout: (a) Layout scheme of sensors on typical longitudinal section; (b) The sensor layout at the test site.

2.4. Spatio-Temporal Distribution Modeling Method

After the pre-test and expert guidance, considering the main growing space of greenhouse crops, we choose 1~8 measurement points of temperature, humidity, light intensity, and CO₂ concentration for 3D distribution reconstruction when analyzing the spatio-temporal distribution of environmental parameters in our greenhouse. The temperature measurement point area is shown in Figure 6. The areas of humidity, light intensity, and CO₂ concentration are shown in Figure 7.

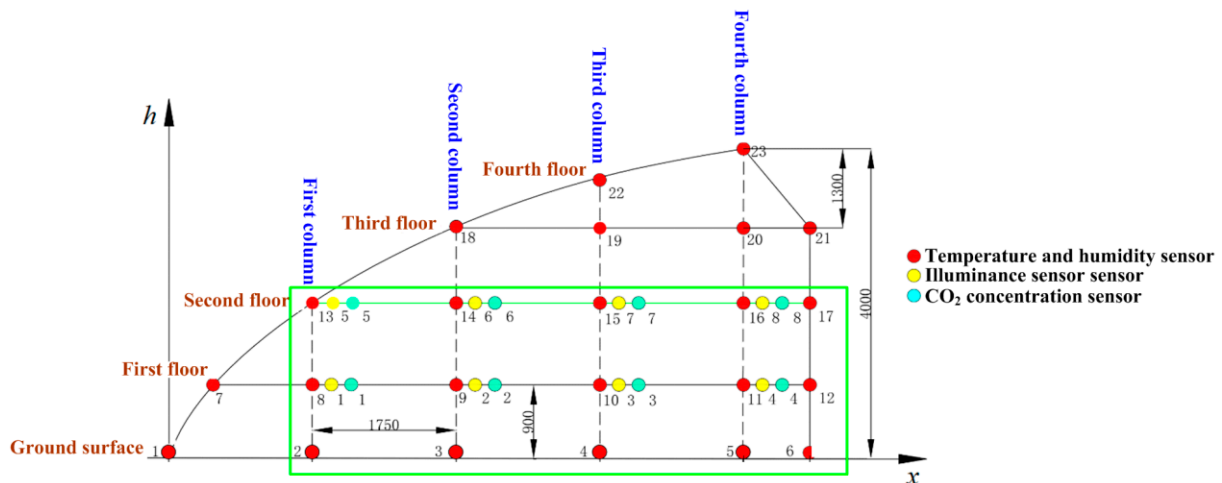


Figure 6. Temperature measurement point area.

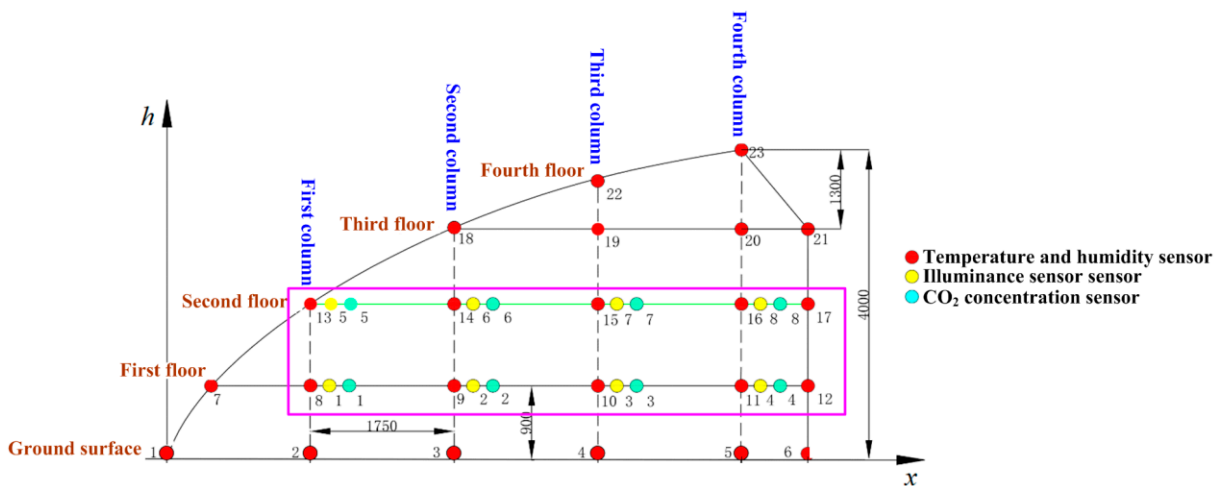


Figure 7. The areas of humidity, light intensity, and CO₂ concentration.

We used Matlab software to model the main growing spaces of crops in the greenhouse based on the measured data. An infinitely refined 3D matrix was used to simulate the distribution of environmental parameters at the measurement points inside the greenhouse. For the data collected at each measurement point, we used Spline (three-dimensional spline interpolation) to obtain a smooth interpolation distribution curve; meanwhile, since the environmental parameter field is the environmental parameter variation on the plane of the analyzed measurement point, we used Interp2 (two-dimensional interpolation) to process the data and used the third dimensional height value and the continuous change of color to represent the continuous change of environmental parameters.

By reviewing the relevant literature and the characteristics of the actual changes of environmental parameters in the greenhouse, a set of instantaneous environmental parameter data was selected as the test value every 3 h from the 24 h monitoring data throughout the day for a total of 9 sets, and a three-dimensional image that can visually reflect the distribution patterns of ambient temperature field, ambient humidity field, light intensity field, and CO₂ concentration field in the test area of the greenhouse was reconstructed according to the spatial location of each measurement point.

3. Results and Discussion

3.1. Horizontal Data Analysis Results

3.1.1. Temperature and Humidity

We selected three test periods in winter, from 10 January to 12 January, 18 January to 21 January, and 22 January to 24 January for indoor temperature and humidity analysis and plotted the daily variation curves of indoor temperature and humidity at each measurement point, as shown in Figures 8 and 9. From Figure 8, it can be seen that the ambient temperature inside the greenhouse was significantly higher than the outdoor temperature at any time, and the maximum indoor temperature was 33.3~44.6 °C, reflecting the strong heat storage and insulation capacity of the greenhouse. From Figure 9, it can be observed that the indoor and outdoor humidity values are basically the same during the process of cotton curtain closing, while during the time period when the cotton curtain is open, the indoor humidity is higher than the outdoor temperature, and the highest indoor humidity can reach 100%, which is more beneficial to the growth of crops in the greenhouse. Meanwhile, the change trend of ambient temperature and humidity on the same height plane in the greenhouse was the same as that of the outdoor temperature and humidity parameters, but the change trend between indoor temperature and humidity was completely opposite, showing a significant negative correlation. It was found that during the process of opening and closing the cotton curtain in the greenhouse, the indoor ambient temperature and humidity changed significantly, and there was a large fluctuation during the time of opening the cotton curtain; there was no significant fluctuation during the time of closing the cotton curtain, and the temperature showed a gradual decrease with time, while the humidity showed a rapid increase, and the humidity at most measurement points was close to the saturation value. This shows that the influence of light intensity on the indoor environment temperature and humidity plays a key role, and that there is a strong coupling relationship between the three.

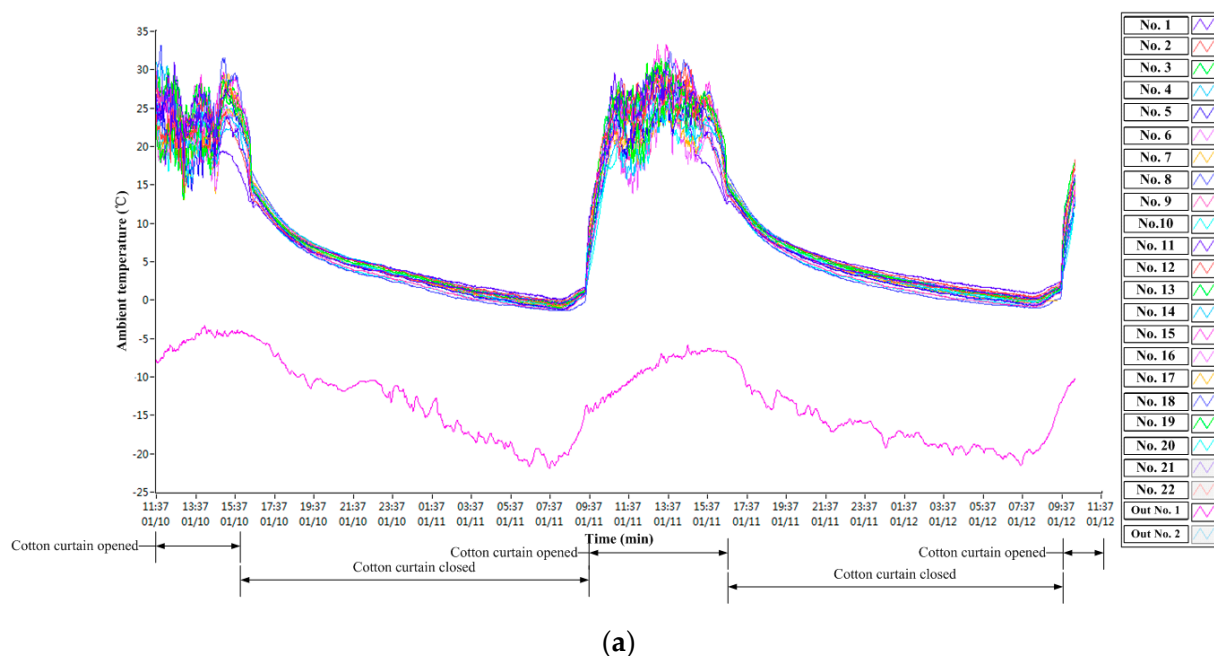
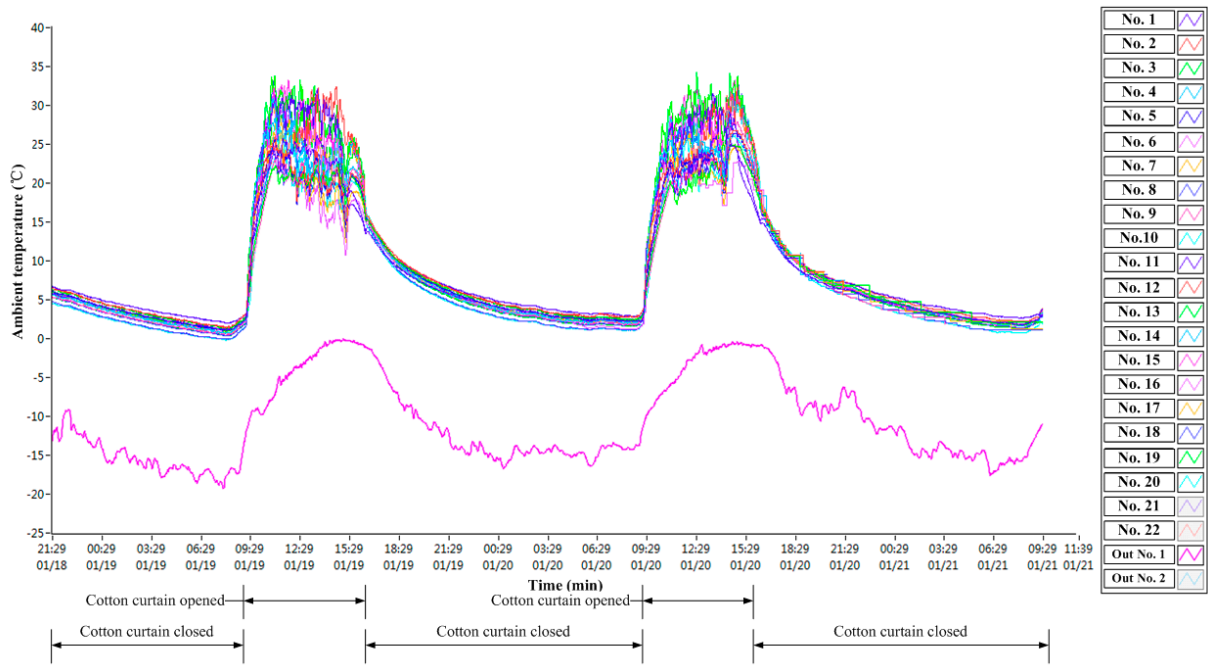
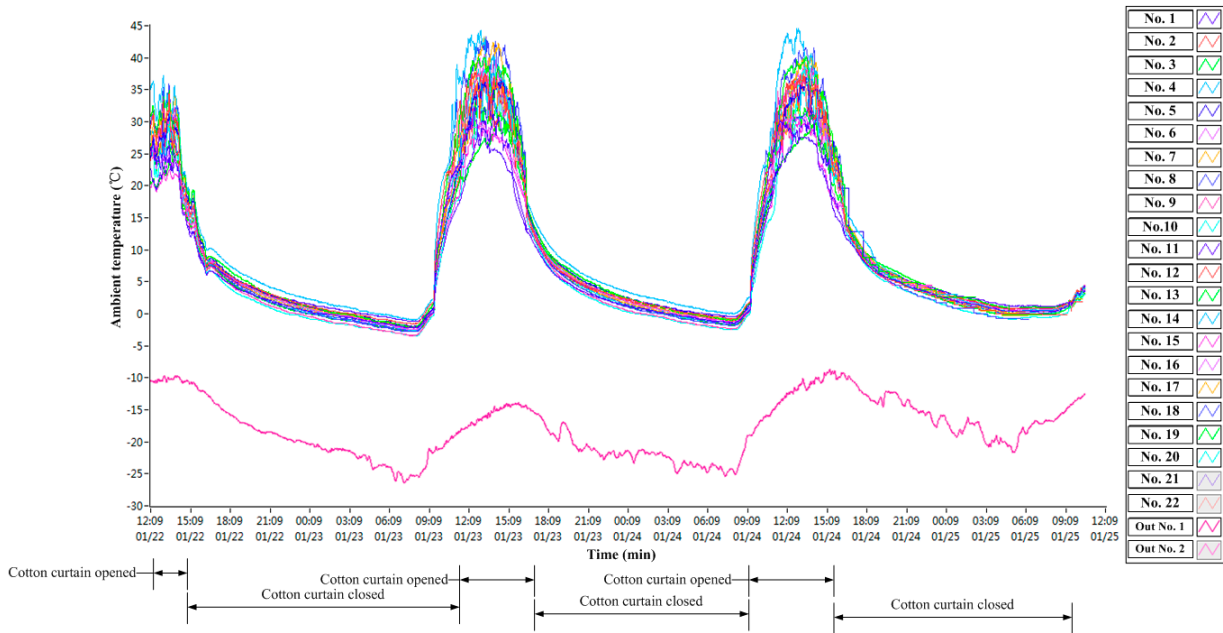


Figure 8. Cont.



(b)



(c)

Figure 8. Circadian change curves of ambient temperature in the horizontal direction: (a) 1/10~1/12; (b) 1/18~1/21; (c) 1/22~1/24.

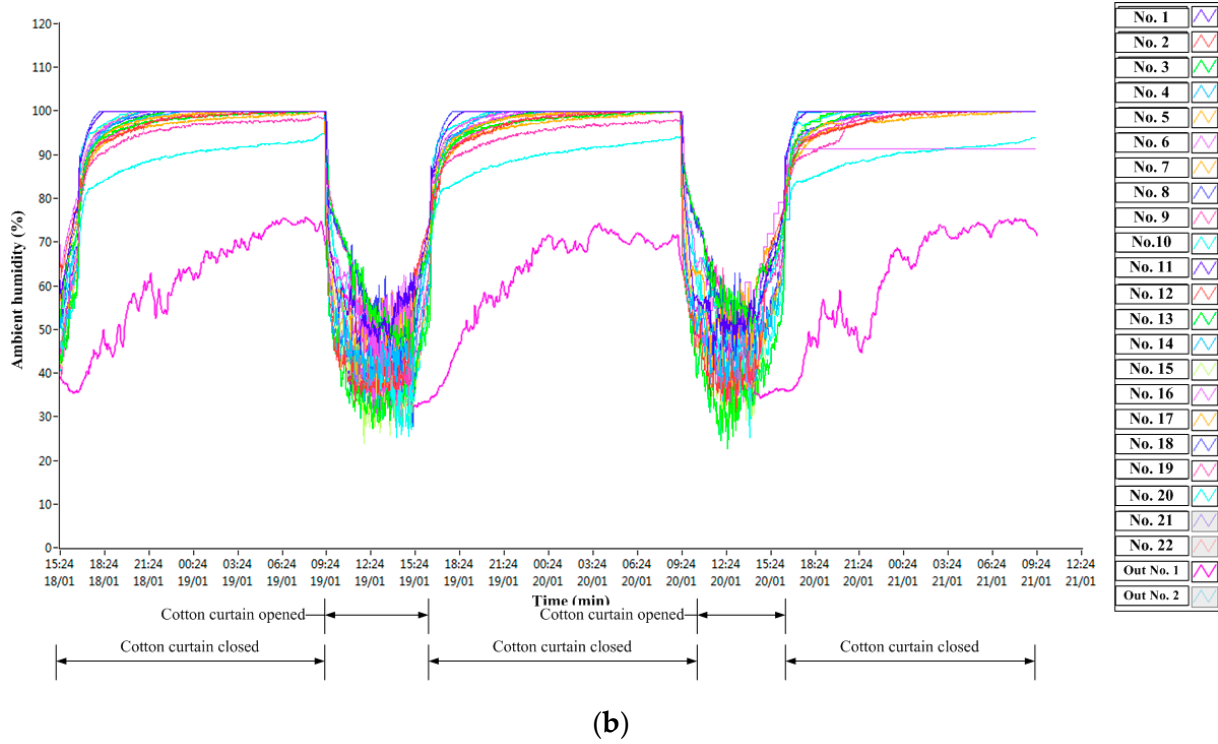
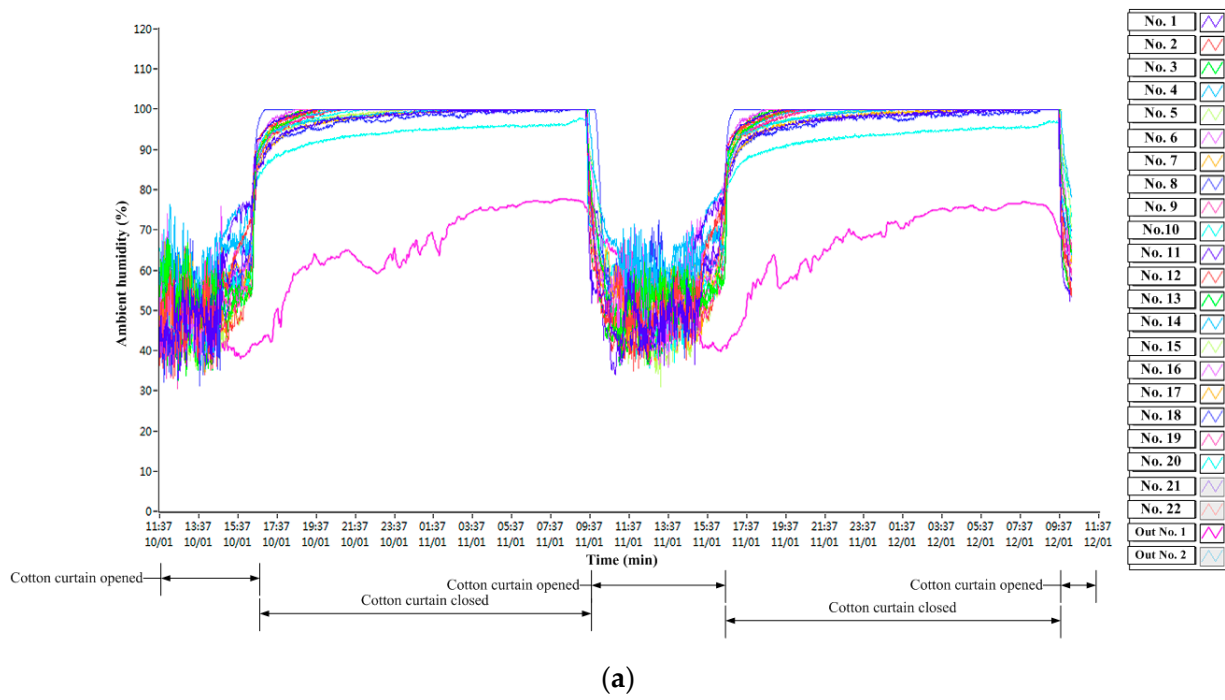


Figure 9. Cont.

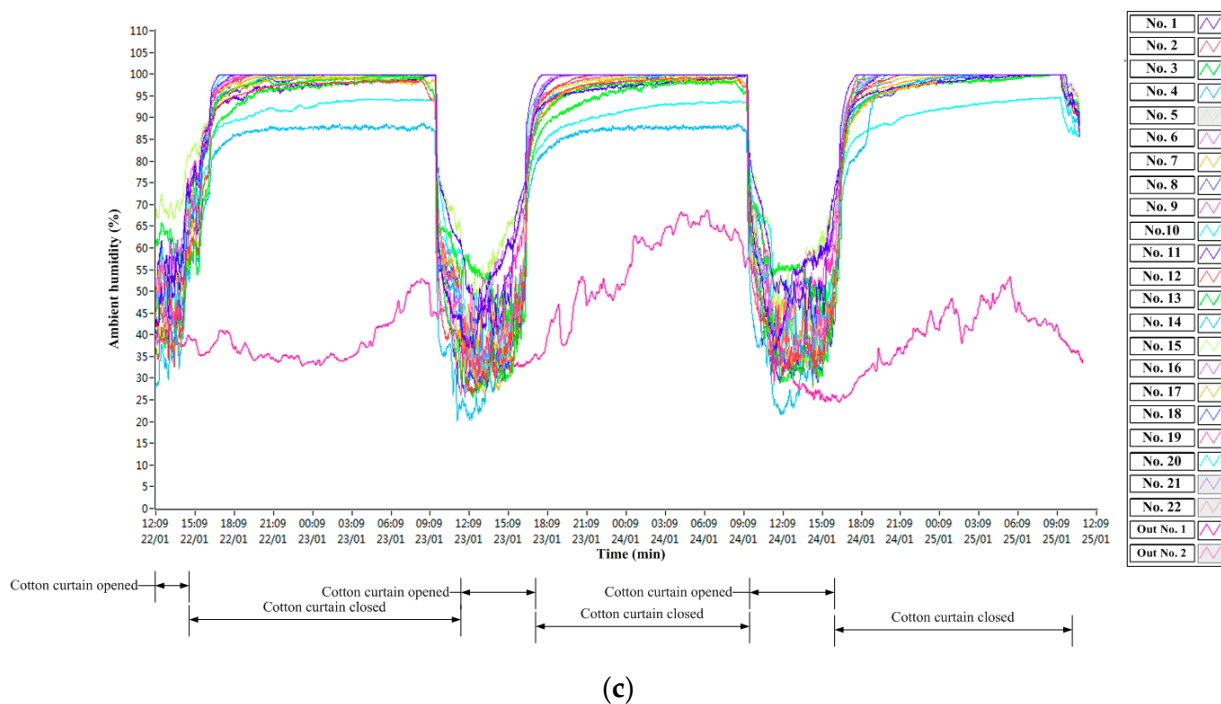


Figure 9. Circadian change curves of ambient humidity in the horizontal direction: (a) 1/10~1/12; (b) 1/18~1/21; (c) 1/22~1/24.

3.1.2. Light Intensity

Three test periods, 10 January to 12 January, 18 January to 20 January, and 22 January to 24 January, were selected for light intensity analysis, and the daily variation curves of light intensity at each measurement point were plotted, as shown in Figure 10. From Figure 10, it can be seen that the light intensity has a significant daily variation pattern. In winter, the whole day light time in the greenhouse is about 7 h, and the cotton curtain is usually opened in winter from 9:30 to 16:30. When the curtain is opened at 9:30, the crop starts photosynthesis, the light intensity increases linearly from 9:30 to 11:30, and the growth rate decreases from 11:30 to 12:00 due to the decrease of CO₂ concentration. The rate of growth decreases and reaches a maximum at 13:30, with a light intensity value of about 65 kLux. The time between 14:00–16:30 shows a linear decrease, and the cotton curtain is closed at about 16:30. Meanwhile, due to the orientation of solar radiation and the shading of the wall in the east–west direction, the east is weak and the west is strong before noon, the east is strong and the west is weak after noon, and the middle of the greenhouse is the best area of light throughout the day. However, the outer middle of the greenhouse is the travel position of the cotton curtain motor and there is shading; therefore, the installation position of the cotton curtain motor can be optimized in subsequent research to expand the light area of the heliostat.

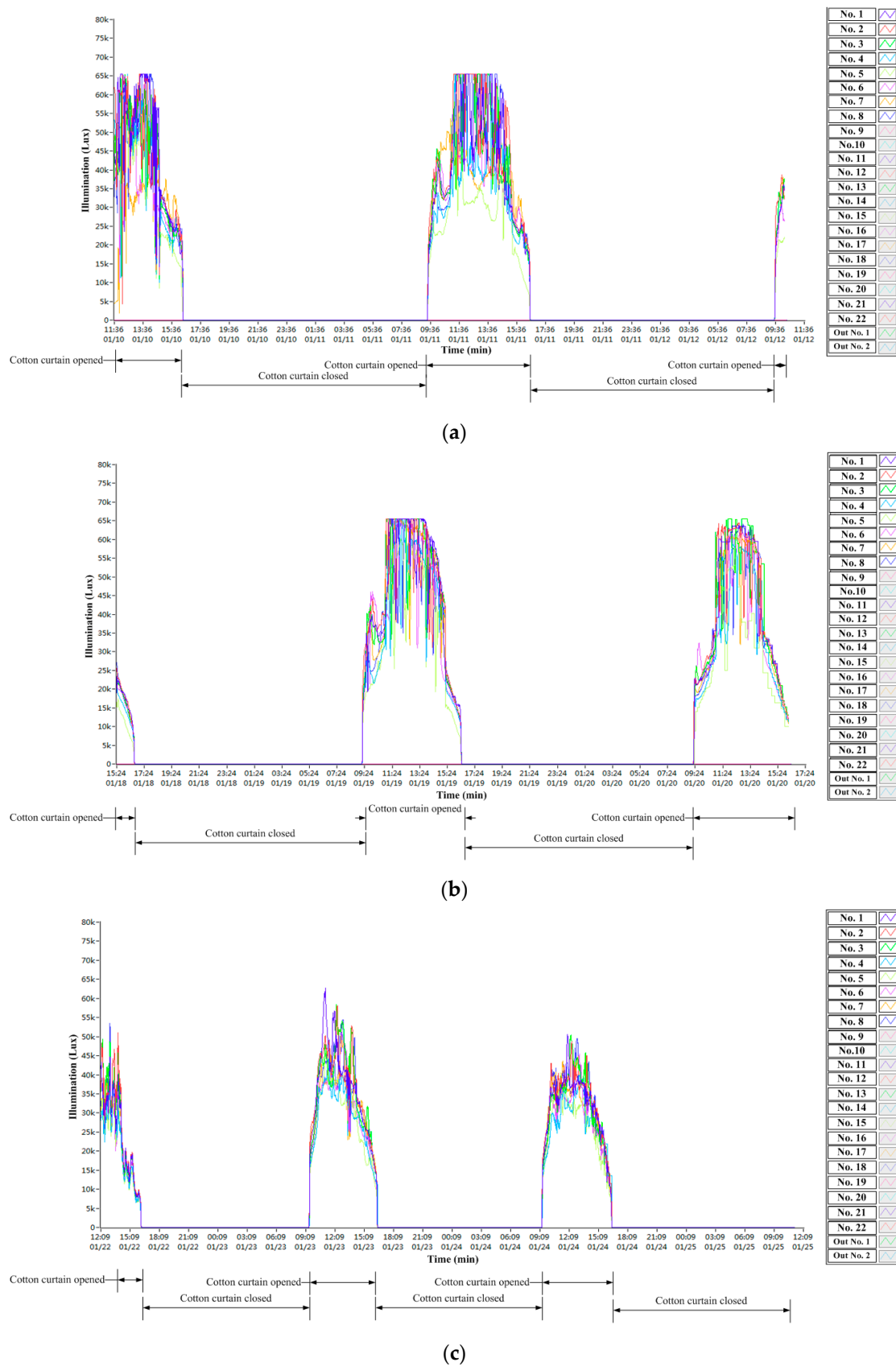


Figure 10. Circadian change curves of light intensity in the horizontal direction: (a) 1/10~1/12; (b) 1/18~1/20; (c) 1/22~1/24.

3.1.3. CO₂ Concentration

Similarly, three test periods were selected for CO₂ concentration analysis in winter: from 10 January to 12 January, from 18 January to 20 January, and from 22 January to 24 January. The daily variation curves of CO₂ concentration at each measurement point were plotted, as shown in Figure 11. From Figure 11, it can be seen that the CO₂ concentration had a significant daily variation pattern. During the time when the cotton curtain was closed, the CO₂ concentration showed a monotonic increasing trend due to the respiration of plants at night, and the rate of increase gradually became slower with time, up to 854–1163 ppm. After the cotton curtain was opened, the CO₂ concentration in the greenhouse dropped sharply with the consumption of photosynthesis of crops, down to 400 ppm. In general, the trend was opposite to that of the light intensity, and there was a strong coupling relationship between the two. This is consistent with the findings of Zhao et al. [2] on light intensity and CO₂ concentration in tomato cultivation in a heliostat.

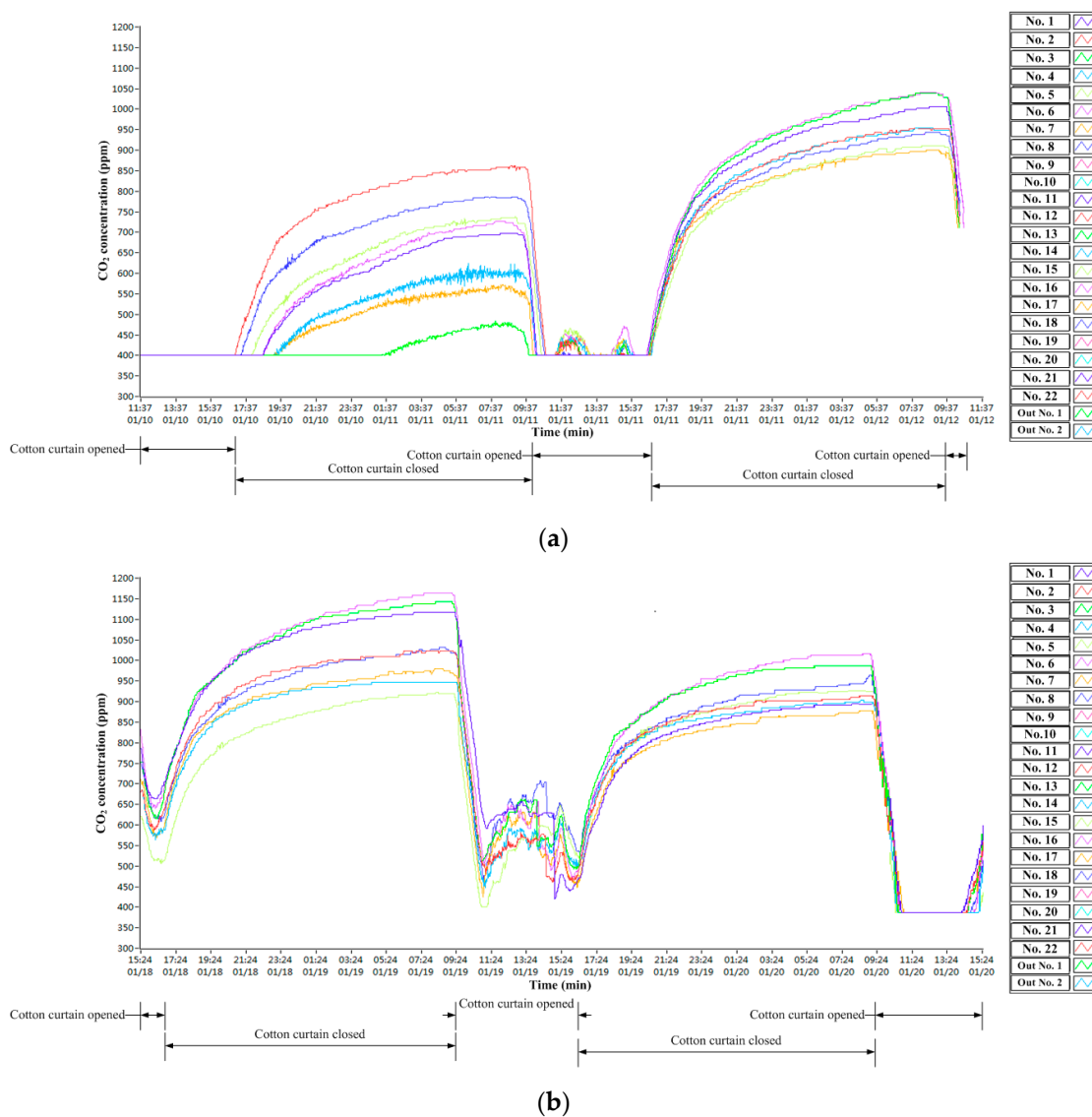


Figure 11. Cont.

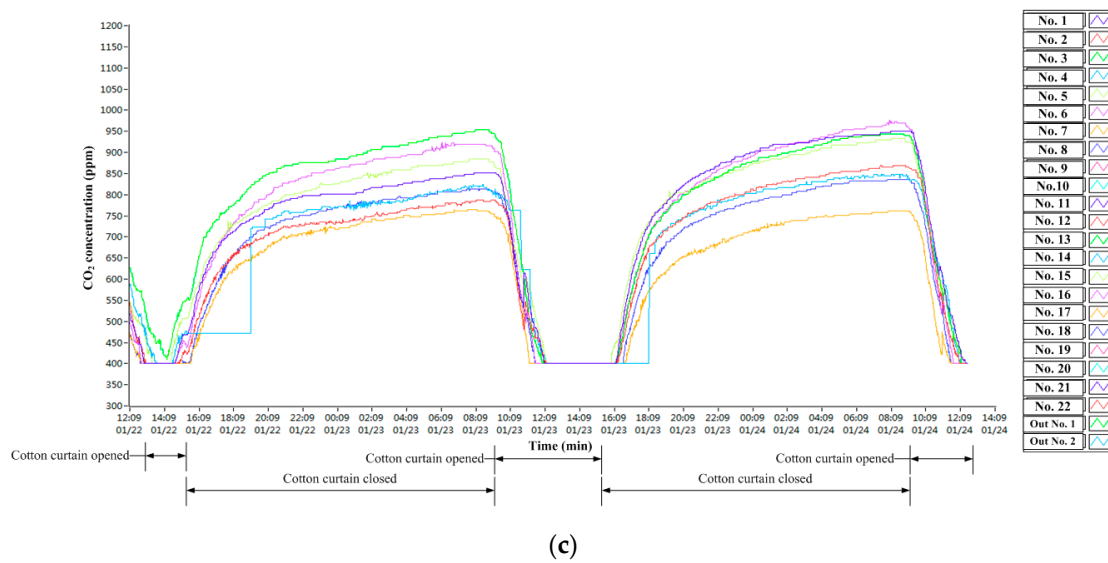


Figure 11. Circadian change curves of CO₂ concentration in the horizontal direction: (a) 1/10~1/12; (b) 1/18~1/20; (c) 1/22~1/24.

3.2. Vertical Data Analysis Results

3.2.1. Temperature and Humidity

Temperature and humidity measurement points were laid out according to the vertical layout scheme (Figures 6 and 7). The daily variation curves of temperature and humidity and outdoor temperature and humidity at each measurement point from 30 January to 2 February 1~8 were plotted, as shown in Figure 12. It was found that the daily change trends of temperature and humidity in the vertical direction were basically the same and that they were the same as the daily change trends in the horizontal direction. Meanwhile, the indoor and outdoor ambient temperature and humidity change trends were consistent, but the indoor temperature and humidity changes were delayed in time.

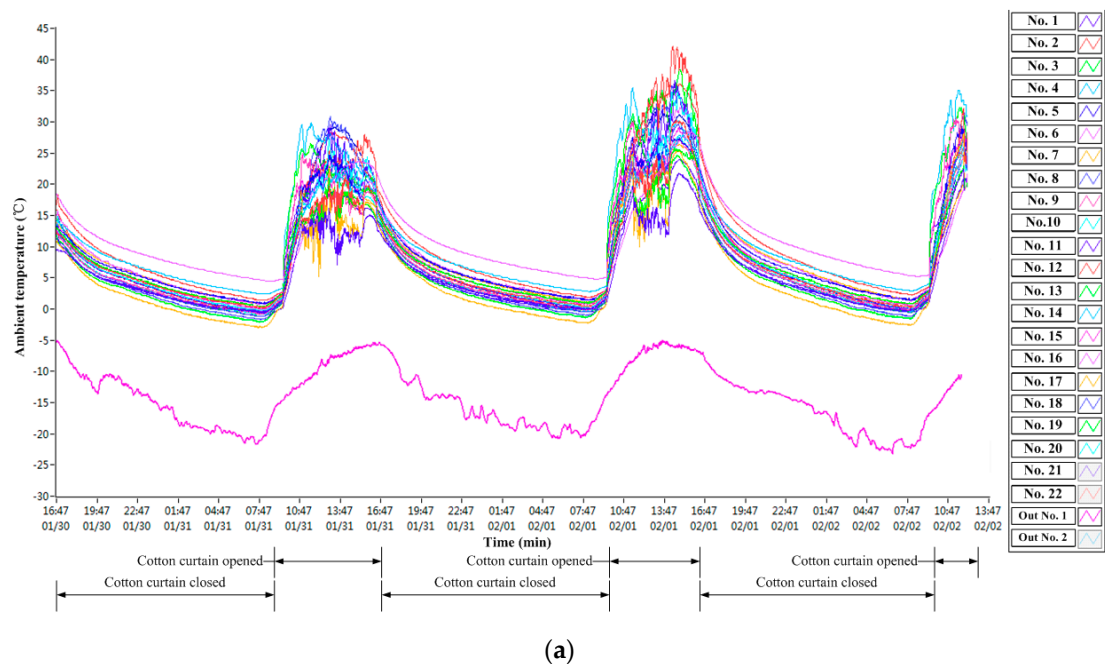


Figure 12. Cont.

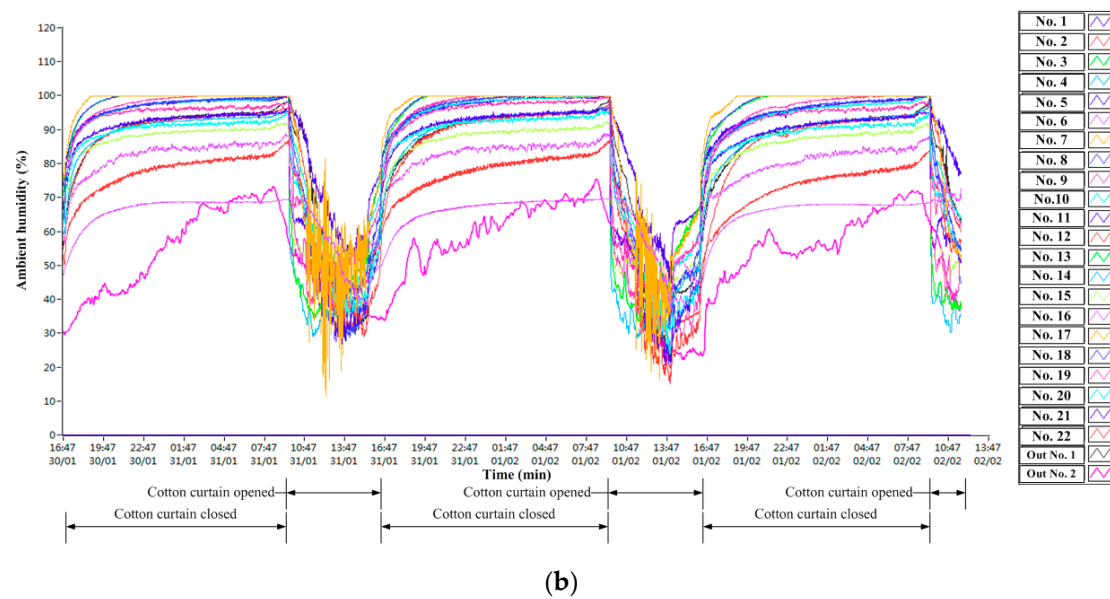


Figure 12. Temperature and humidity daily change curve in vertical direction: (a) Temperature; (b) Humidity.

The same 3D modeling scheme for environmental parameters was used to reconstruct the 3D distribution of temperature and humidity at each measurement point from one to eight and the outdoor temperature and humidity. The 3D images of the spatial and temporal distributions of temperature and humidity on 1 February are plotted as shown in Figure 12. It can be seen that the indoor ambient temperature changed at 0:00, 3:00, and 6:00, showing a gradually decreasing trend; at 6:00, 9:00, 12:00, and 15:00, showing a gradually increasing trend; and at 15:00, 18:00, 21:00, and 24:00, showing a gradually decreasing trend. Among the 3D images corresponding to the nine time points analyzed, the highest overall ambient temperature was found at 15:00, while the lowest overall ambient temperature was found at 6:00. The magnitude of ambient temperature change in the measured area at different times and spaces was slightly different, and the longitudinal ambient temperature distribution in the longitudinal section was significantly uneven during the time when the cotton curtain was open, while the distribution was relatively uniform during the time when the cotton curtain was closed. From 0:00, 3:00, and 6:00 to 9:00, the indoor ambient humidity showed a gradually rising trend; the values were very high and the differences were very small; all values were saturated or close to saturation. From 9:00 to 12:00 to 15:00, ambient humidity showed a gradually decreasing trend; from 15:00, 18:00, and 21:00 to 24:00, ambient humidity changes showed a gradually rising trend again. Among the 3D images corresponding to the nine time points analyzed, the overall ambient humidity at 15:00 was the lowest. During the time when the cotton curtain was open, the longitudinal humidity distribution in the longitudinal section was not uniform to a significant degree, and the gradient between the measured points was large. The magnitude of ambient humidity changes at different times and in different spaces in the measured area varied, and near the rear wall side the ambient humidity decreased significantly. Comparing Figure 13a,b, it can be seen that there is a significant negative correlation between ambient temperature and humidity in the greenhouse.

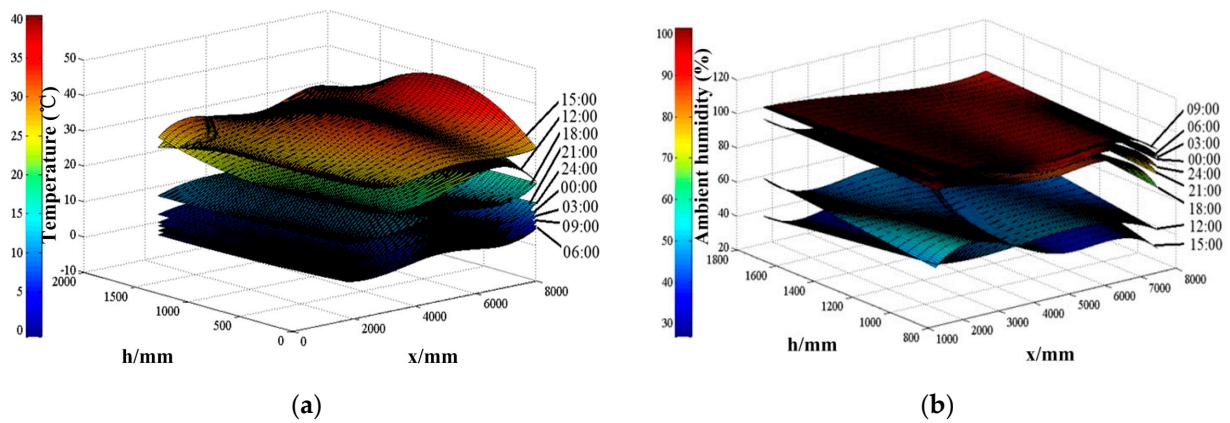


Figure 13. 3D images of spatial and temporal distribution of temperature and humidity: (a) Temperature; (b) Humidity.

3.2.2. Light Intensity

Light intensity measurement points were laid out according to the vertical layout scheme (Figure 7). The daily variation curves of light intensity and outdoor light intensity at each measurement point from 30 January to 2 February 1~8 were selected for analysis, as shown in Figure 14. The overall light intensity variation curves during the test period were plotted, and it was found that the daily variation trend was basically the same on sunny days.

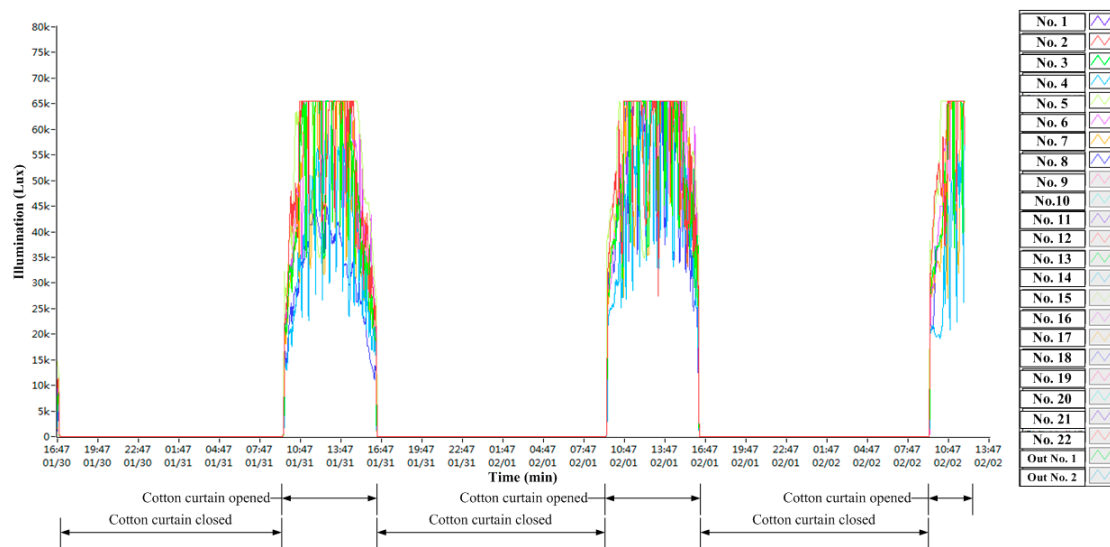


Figure 14. Daily variation curve of light intensity in vertical direction.

Considering that the indoor light intensity was zero during the time when the greenhouse cotton curtain was closed, the instantaneous light intensity at 1-h intervals was used as the test value from 10:00 to 16:00 every day during the test period. The three-dimensional images of the spatial and temporal distribution of light intensity on one of the days (1 February) were selected for analysis, as shown in Figure 15. During the time when the cotton curtain was closed, the indoor light intensity was zero because no supplemental light measures were taken, and during the time when the cotton curtain was open, the light intensity at each measurement point changed sharply within a partially short period of time due to the change of the solar incidence angle, the curvature of the front roof of the greenhouse, the uneven light transmission of the film, and the shading of the clouds. In general, the distribution of light intensity in the greenhouse from south to north showed a

trend of high distribution in the central part and low distribution in the north and south, and the uniformity was poor. The highest light intensity was basically during the range of 12:00 to 14:00. Considering that crops can be damaged by strong light and the problem of high ambient temperature in the greenhouse due to excessive light, appropriate ventilation and shading measures should be taken in greenhouses even during the period of 11:00 to 15:00 on sunny days during the high cold period in winter. Therefore, in the follow-up study, it will be necessary to investigate the curvature and light transmission of the film at different positions on the front roof of the greenhouse to optimize the structure of the greenhouse and improve the uniformity of the indoor light intensity distribution.

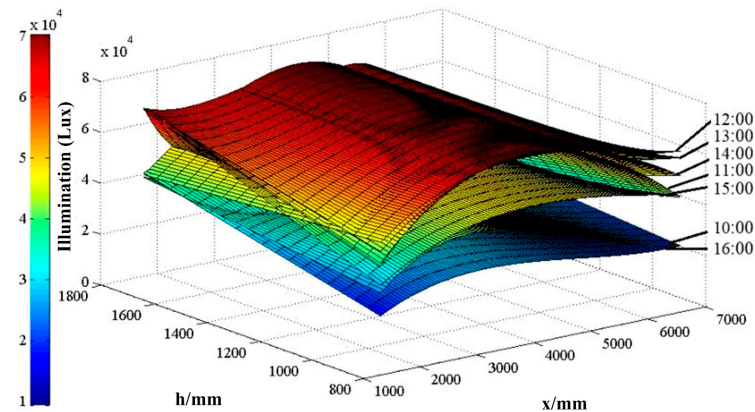


Figure 15. 3D images of spatial and temporal distribution about light intensity.

3.2.3. CO₂ Concentration

The CO₂ concentration measurement points were laid out according to the vertical layout scheme (Figure 7). The daily variation curves of CO₂ concentration and outdoor CO₂ concentration at each measurement point from 30 January to 2 February were plotted, as shown in Figure 16, and their daily variation trends were basically the same.

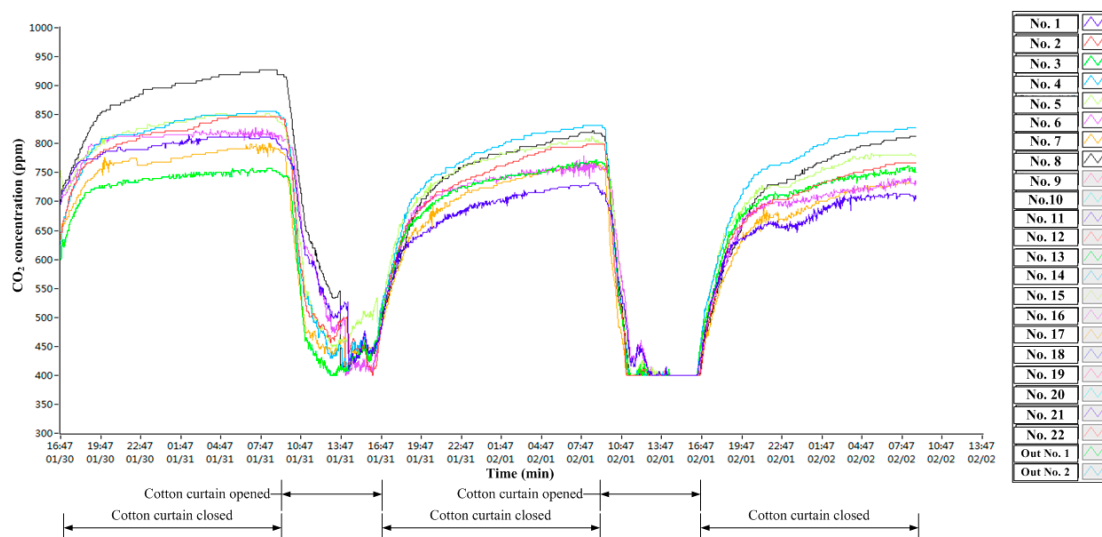


Figure 16. Daily variation curve of CO₂ concentration in vertical direction.

The same three-dimensional modeling scheme for environmental parameters was used to reconstruct the three-dimensional distribution of CO₂ concentration at measurement points one to eight. Considering that the data of some measurement points were truncated due to the range of the CO₂ concentration sensor during the experiment, the 3D image of the spatial and temporal distribution of CO₂ concentration on the day with good data

integrity (February 1) was selected for analysis. The results are shown in Figure 17. The results show that the three-dimensional images of the daily distribution show basically the same pattern. During the time when the cotton curtain was opened (9:30~4:47), the CO₂ concentration at 15:00 was generally significantly lower than that at 12:00; the amplitude of the fitted surface at 12:00 was more variable and was significantly influenced by the light intensity; during the time when the cotton curtain was closed (4:47~9:30), the indoor CO₂ concentration distribution generally showed a pattern of high distribution at the north and south sides and low distribution at the middle part, and the CO₂ concentration increased with time and the fluctuation amplitude also increased, which also indicated that there was still a close relationship between indoor CO₂ concentration and other environmental parameters except for light intensity.

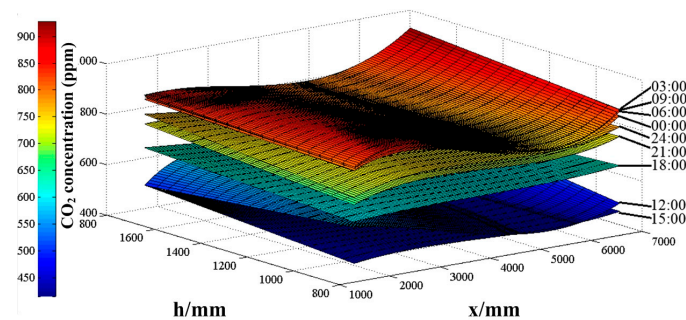


Figure 17. 3D images of spatial and temporal distribution of CO₂ concentration.

3.3. Coupling Model of Solar Greenhouse Environmental Parameters

In order to improve the accuracy of modeling, the data of environmental parameters at each measurement point of multiple tests were selected to be averaged from 17:00 on 31 January to 17:00 on 1 February. That is 2880 min. Then, the CO₂ concentration–light intensity–time and the CO₂ concentration–light intensity–indoor temperature models were constructed to analyze the coupling relationship between the parameters and the main factors affecting the distribution conditions and the change patterns of the indoor environmental parameters.

3.3.1. Model of CO₂ Concentration–Light Intensity–Time

The model of CO₂ concentration ($f(x, t)$)–light intensity (x)–time (t) was constructed through averaging the monitoring data of the measuring points in the same period. The fitting results are shown in Figure 18, and the mathematical models of each measuring point are shown in Table 1.

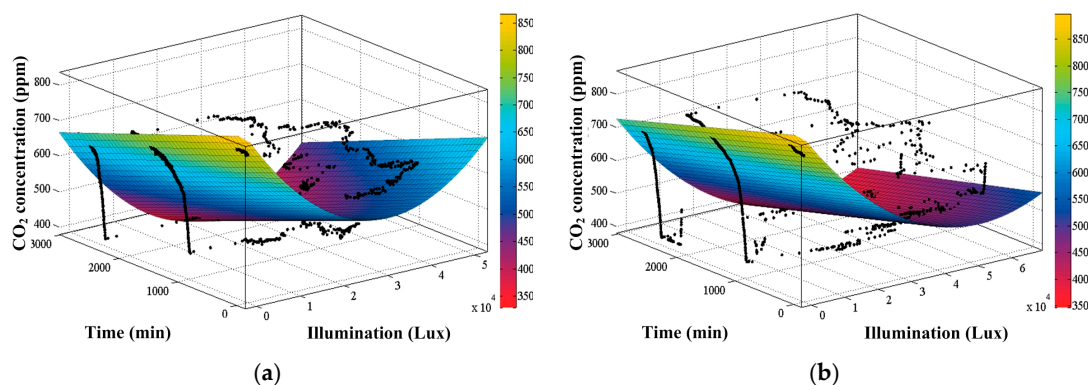


Figure 18. Cont.

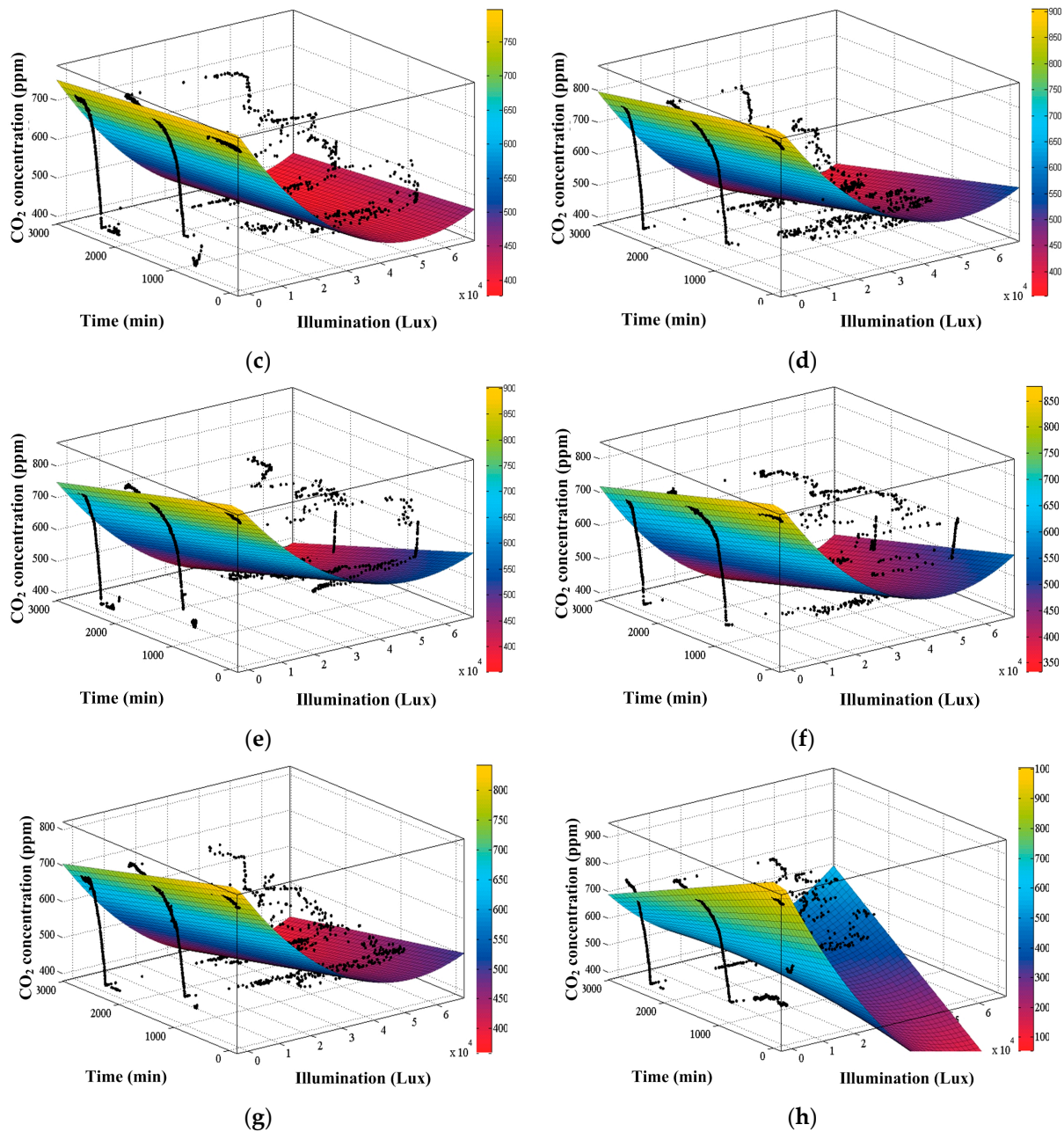


Figure 18. CO₂ concentration model 1 at each measuring point: (a) No. 1 measuring point; (b) No. 2 measuring point; (c) No. 3 measuring point; (d) No. 4 measuring point; (e) No. 5 measuring point; (f) No. 6 measuring point; (g) No. 7 measuring point; (h) No. 8 measuring point.

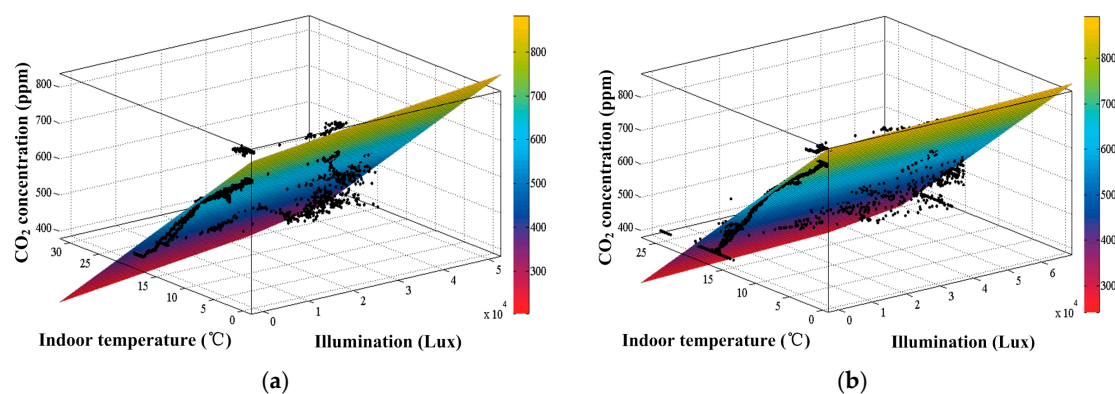
Table 1. Fitting models of indoor CO₂ concentration–light intensity–time.

Measuring Point	Fitting Equation	Regression Coefficient (R ²)	RMSE (ppm)
1	$f(x, t) = 807.1 - 0.01841x - 0.06285t + 3.069 \times 10^{-7}x^2 - 1.45 \times 10^{-7}xt$	0.88	45.06
2	$f(x, t) = 841.6 - 0.01389x - 0.05439t + 1.394 \times 10^{-7}x^2 + 1.034 \times 10^{-7}xt$	0.90	49.67
3	$f(x, t) = 750.7 - 0.01314x - 0.0138t + 1.298 \times 10^{-7}x^2 + 8.259 \times 10^{-7}xt$	0.95	31.37
4	$f(x, t) = 849.3 - 0.01448x - 0.03431t + 1.453 \times 10^{-7}x^2 - 2.108 \times 10^{-7}xt$	0.93	42.13
5	$f(x, t) = 851.3 - 0.01278x - 0.04859t + 1.266 \times 10^{-7}x^2 - 1.926 \times 10^{-7}xt$	0.93	39.45
6	$f(x, t) = 820.9 - 0.01442x - 0.05031t + 1.538 \times 10^{-7}x^2 + 1.775 \times 10^{-7}xt$	0.93	38.01
7	$f(x, t) = 791.6 - 0.01272x - 0.04242t + 1.231 \times 10^{-7}x^2 + 1.552 \times 10^{-7}xt$	0.92	38.98

It can be seen from Figure 15 and Table 1 that the three-dimensional model of indoor CO₂ concentration, light intensity, and time at eight measuring points shows an obvious non-linear relationship, and the differences are large, which indicates that the CO₂ concentration at different indoor locations has large differences, and the distribution is extremely uneven. The fitting model among the three is relatively complex, but the whole relationship can be expressed by $f(x, t) = a + bx + ct + dx^2 + ext$. The fitting degree is greater than 0.85, and the RMSE (root mean square error) is less than 50 ppm, which indicates that the model basically conforms to the coupling relationship among the three. The coupling between CO₂ concentration and light intensity at each measuring point is strong, because the indoor photosynthesis is enhanced during the opening period of the cotton curtain, and the crop respiration is enhanced during the closing period, which affects the indoor CO₂ concentration change, indicating that the type and layout of indoor crops play a key role in the distribution and change of CO₂ concentration.

3.3.2. Model of CO₂ Concentration–Light Intensity–Indoor Temperature

Use the same method, the model of CO₂ concentration ($f(x, t)$)–light intensity (x)–indoor temperature (y) was constructed. The fitting results are shown in Figure 19, and the mathematical models of each measuring point are shown in Table 2.

**Figure 19.** Cont.

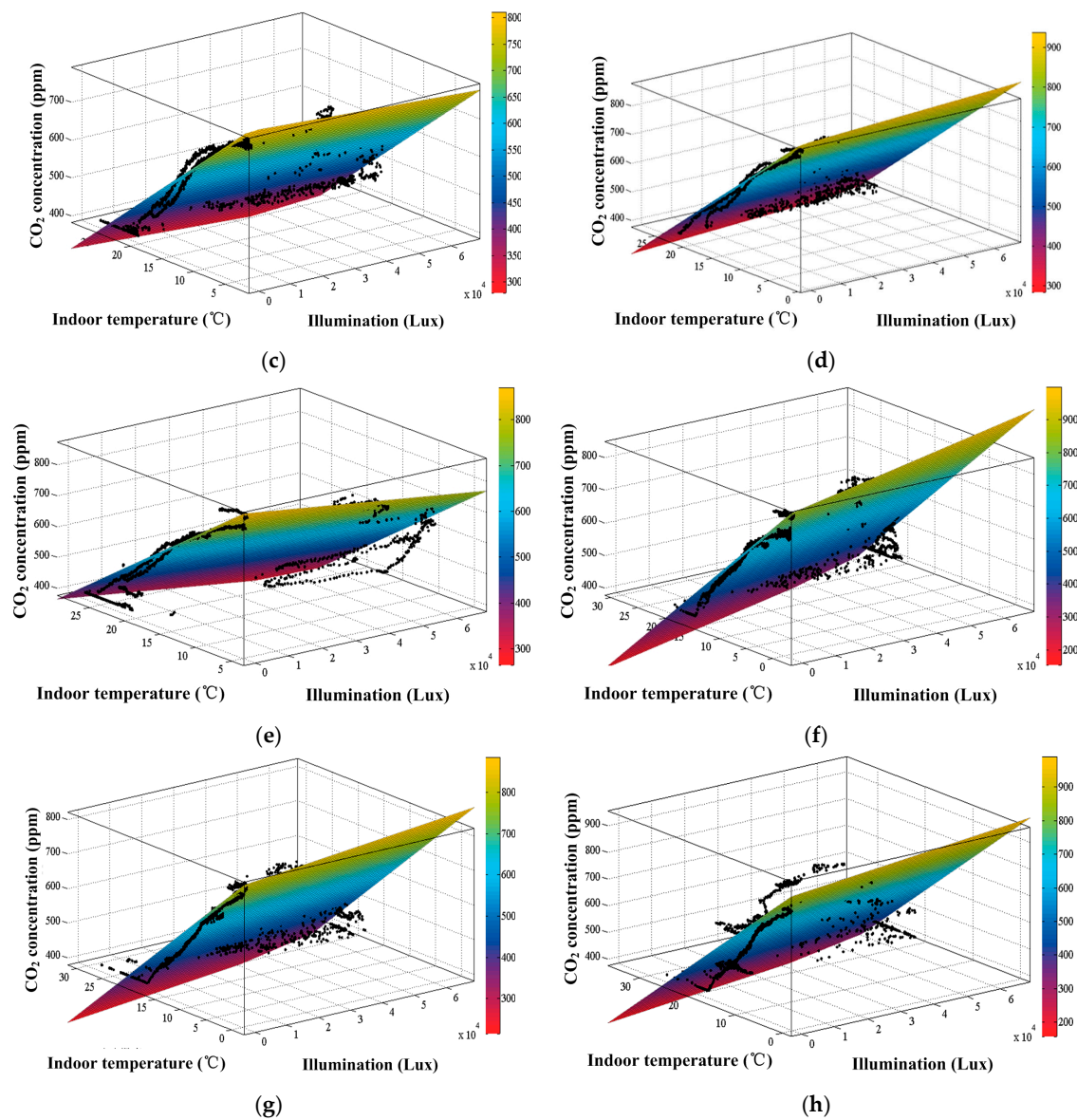


Figure 19. CO₂ concentration model 2 at each measuring point: (a) No. 1 measuring point; (b) No. 2 measuring point; (c) No. 3 measuring point; (d) No. 4 measuring point; (e) No. 5 measuring point; (f) No. 6 measuring point; (g) No. 7 measuring point; (h) No. 8 measuring point.

Table 2. Fitting models of indoor CO₂ concentration–light intensity–indoor environmental temperature.

Measuring Point	Fitting Equation	Regression Coefficient (R ²)	RMSE (ppm)
1	$f(x, y) = 780.7 + 1.466 \times 10^{-3}x - 18.04y$	0.89	43.03
2	$f(x, y) = 848.6 + 3.312 \times 10^{-4}x - 22.39y$	0.95	35.28
3	$f(x, y) = 826.6 + 4.792 \times 10^{-4}x - 17.61y$	0.96	29.02
4	$f(x, y) = 886.1 + 6.119 \times 10^{-4}x - 20.76y$	0.98	25.1
5	$f(x, y) = 927.9 - 1.39 \times 10^{-3}x - 19.23y$	0.91	45.30
6	$f(x, y) = 786.2 + 2.12 \times 10^{-3}x - 20.06y$	0.93	38.36
7	$f(x, y) = 774.3 + 9.642 \times 10^{-4}x - 17.56y$	0.93	35.86

It can be seen from Figure 16 and Table 2 that the model can be expressed by $f(x, y) = a + bx + cy$, and the fitting degree of the curve is greater than 0.89, indicating that compared with CO₂ concentration ($f(x, t)$)–light intensity (x)–time (t), this model is more consistent with the coupling relationship; furthermore, in addition to the light intensity, the indoor environmental temperature also has a significant effect on CO₂ concentration.

4. Conclusions

(1) According to the results of the horizontal and vertical measurements of temperature, humidity, light intensity, and CO₂ concentration in the heliostat, the temperature, humidity, light intensity, and CO₂ concentration in the room had a significant daily variation pattern. In the east–west direction of the greenhouse, the light intensity was weak in the east and strong in the west before noon, strong in the east and weak in the west after noon, and the central part of the greenhouse was the best light area throughout the day. The horizontal spatial distribution of CO₂ concentration in the greenhouse was basically the same. According to the distribution of light intensity, it is recommended to plant light-loving crops in the middle of the greenhouse for a reasonable layout of the greenhouse as a planting structure.

(2) The trends of ambient temperature inside the greenhouse and of outdoor temperature were basically the same, the overall indoor temperature was significantly higher than the outdoor temperature, and the overall trend of indoor temperature increased from south to north. The overall trend of indoor ambient temperature gradually decreased from bottom to top. The indoor and outdoor humidity were basically the same during the time when the cotton curtain was closed, and during the time when the cotton curtain was open the indoor humidity was higher than the outdoor temperature, up to 100%. For the northern cold and arid areas, the north–east and north–west winds dominate in autumn and winter, and the temperature in the central space of the greenhouse is obviously high, so cooling measures should be taken for the central space of the greenhouse under natural ventilation in autumn and winter.

(3) The indoor CO₂ concentration showed an increasing trend during the time when the cotton curtain was closed, i.e., when the light intensity was zero. During the time when the cotton curtain was open, i.e., when the light intensity was not zero, the CO₂ concentration dropped sharply. Overall, there was an obvious non-linear relationship between light intensity, CO₂, and time. Meanwhile, the indoor light intensity also had a significant effect on the ambient temperature and CO₂ concentration.

(4) The coupled models of indoor light intensity–CO₂ concentration–time and indoor temperature–light intensity–CO₂ concentration were established, the coefficients of determination (R^2) were obtained as 0.88 and 0.89, and the standard errors (RMSE) were 49.67 ppm and 45.30 ppm, respectively. The model fitting accuracy was high. Therefore, the model constructed in the study can characterize the temperature, light intensity, and CO₂ concentration in the greenhouse more accurately, which can provide an important theoretical basis for greenhouse environmental regulation.

Author Contributions: Conceptualization, C.Z., H.L. and Z.Z.; methodology, C.Z. and H.L.; software, H.W.; validation, C.Z., H.L. and X.Z.; formal analysis, S.W.; investigation, X.Z. and Y.L.; resources, C.W. and Z.Z.; data curation, H.W.; writing—original draft preparation, C.Z., H.L. and X.Z.; writing—review and editing, C.W., Z.Z. and S.W.; visualization, H.W., S.W. and Y.L.; supervision, C.W. and Z.Z. All authors have read and agreed to the published version of the manuscript.

Funding: This research received no external funding.

Institutional Review Board Statement: Not applicable.

Informed Consent Statement: Not applicable.

Conflicts of Interest: The authors declare no conflict of interest.

References

1. Miao, X. Talking about facility horticulture engineering and China's agricultural modernization. *Xin NongCun* **2018**, *21*, 135.
2. Zhao, J.; Li, Z.; Wang, W.; Li, J.; Cao, R. Spatial and temporal distribution test and analysis of tomato planting environment parameters in solar greenhouse. *J. Shanxi Agric. Sci.* **2019**, *47*, 2172–2176+2181.
3. Cheng, X. Predication and CFD Modeling for Greenhouse Microclimates Temporospatial Distributions. Ph.D. Thesis, Jiangsu University, Zhenjiang, China, 2011.
4. Li, M.; Chen, S.; Liu, F.; Zhao, L.; Xue, Q.; Wang, H.; Chen, M.; Lei, P.; Wen, D.; Antonio Sanchez-Molina, J.; et al. A risk management system for meteorological disasters of solar greenhouse vegetables. *Precis. Agric.* **2017**, *18*, 997–1010. [[CrossRef](#)]
5. Chen, S.; Li, Z.; Liu, F.; Yang, S.; Li, M. Risk evaluation of solar greenhouse cucumbers low temperature disaster based on GIS spatial analysis in Tianjin, China. *Geomat. Nat. Hazards Risk* **2019**, *10*, 576–598. [[CrossRef](#)]
6. Kittas, C.; Karamanis, M.; Katsoulas, N. Air temperature regime in a forced ventilated greenhouse with rose crop. *Energy Build.* **2005**, *37*, 807–812. [[CrossRef](#)]
7. Sethi, V.P. On the selection of shape and orientation of a greenhouse: Thermal modeling and experimental validation. *Solar Energy* **2009**, *83*, 21–38. [[CrossRef](#)]
8. Patil, S.L.; Tantau, H.J.; Salokhe, V.M. Modelling of tropical greenhouse temperature by auto regressive and neural network models. *Biosyst. Eng.* **2008**, *99*, 423–431. [[CrossRef](#)]
9. Hamad, I.H.; Chouchaine, A.; Bouzaouache, H. On modeling greenhouse air-temperature: An experimental validation. In Proceedings of the 18th International Multi-Conference on Systems, Signals & Devices (SSD), Monastir, Tunisia, 22–25 March 2021.
10. Cayli, A. Temperature and relative humidity spatial variability: An assessment of the environmental conditions inside greenhouses. *Fresenius Environ. Bull.* **2020**, *29*, 4954–4962.
11. He, Y.; Xu, H.; Li, T.; Yakakuql, T. The change of Temperature of The Back Wall in Solav Greenhouse and Forecasting Model. *North. Hortic.* **2012**, *1*, 34–39.
12. Yang, X.; Zhuo, B.; Qi, Z. The Vertical and Horizontal Distribution of Temperature in Solar Greenhouse. *Hebei Norm. Univ. J.* **2005**, *29*, 79–84.
13. Le, Z.; Shi, M.; Wei, Q.; Gong, Z.; Li, X. Temperature Variation Characteristics in East-West Direction of Solar Greenhouse with Large Length. *Guizhou Agric. Sci.* **2022**, *50*, 94–102.
14. Zhang, X.; Lv, J.; Xie, J.; Yu, J.; Zhang, J.; Tang, C.; Li, J.; He, Z.; Wang, C. Solar Radiation Allocation and Spatial Distribution in Chinese Solar Greenhouses: Model Development and Application. *Energies* **2020**, *13*, 1108. [[CrossRef](#)]
15. Mobtaker, H.G.; Ajabshirchi, Y.; Ranjbar, S.F.; Matloobi, M. Simulation of thermal performance of solar greenhouse in north-west of Iran: An experimental validation. *Renew. Energy* **2019**, *135*, 88–97. [[CrossRef](#)]
16. LÜ, H.; Niu, Y.; Zhang, M.; Li, H. Analysis of Variation Trend of Light Intensity and Air Temperature and Humidity in Solar Greenhouse. *Trans. Chin. Soc. Agric. Mach.* **2022**, *52*, 410–417.
17. Gao, Q.; Liang, Y.; Duan, A. Light characteristics and its changing laws in solar greenhouse. *Trans. Chin. Soc. Agric. Eng.* **2003**, *19*, 200–204.
18. Tong, G.; Wang, E.; Wang, T.; Meng, S. Test and analysis of indoor environment of Liaoshen Type I solar greenhouse. *Liaoning Agric. Sci.* **2003**, *5*, 11–12.
19. Zhang, Y.; Jung, Y.; Freifeld, B.; Finsterle, S. Using distributed temperature sensing to detect CO₂ leakage along the injection well casing. *Int. J. Greenh. Gas Control* **2018**, *74*, 9–18. [[CrossRef](#)]
20. Yang, Y.; Guo, Y.; Sun, X.; Li, T. Analysis of CO₂ concentration change of long-season tomato cultivation in solar greenhouse. *J. Shenyang Agric. Univ.* **2000**, *31*, 82–85.
21. Assadi-Langroudi, A.; O'Kelly, B.C.; Barreto, D.; Cotecchia, F.; Dicks, H.; Ekinci, A.; Garcia, F.E.; Harbottle, M.; Tagarelli, V.; Jefferson, I.; et al. Recent Advances in Nature-Inspired Solutions for Ground Engineering (NiSE). *Int. J. Geosynth. Ground Eng.* **2022**, *8*, 3. [[CrossRef](#)]

Disclaimer/Publisher's Note: The statements, opinions and data contained in all publications are solely those of the individual author(s) and contributor(s) and not of MDPI and/or the editor(s). MDPI and/or the editor(s) disclaim responsibility for any injury to people or property resulting from any ideas, methods, instructions or products referred to in the content.